

First-Order, Structural Transformations in Metallic Glasses

B. W. Corb,^(a) R. C. O'Handley, J. Megusar, and N. J. Grant

*Department of Materials Science and Engineering and Center for Materials Science and Engineering,
Massachusetts Institute of Technology, Cambridge, Massachusetts 02139*

(Received 10 December 1982; revised manuscript received 11 July 1983)

Magnetic evidence is presented for a first-order, structural transformation in the local order of a cobalt-base metallic glass. The transformation is centered at $T_0 = 180^\circ\text{C}$ and shows a scan-rate-dependent thermal hysteresis of $\Delta T = 100^\circ\text{C}$. A critical volume for nucleation of the transformation is estimated to contain approximately 200 atoms. The transformation appears in samples which show no microcrystallites greater than 30 \AA and vanishes in samples with appreciable crystallinity. The observations are discussed in terms of model clusters of icosahedral, trigonal, and octahedral symmetry.

PACS numbers: 81.30.Kf, 71.25.Mg, 75.50.Kj

The current view of the structure of metallic glasses—the quasicrystalline model—considers them to be assembled of randomly oriented atomic clusters whose short-range order (SRO) often approaches that of a related crystalline phase.¹ For some metallic glasses two distinct SRO's have been shown to coexist simultaneously, either as phase separation² or as polymorphism.³ It has been proposed that it may be possible to observe a reversible transformation from one SRO to another in some glasses.⁴

In this Letter we describe what we believe to be the first observation—albeit indirect—of such a transformation in a glassy alloy. The transformation, observable in a cobalt-base amorphous alloy as a thermomagnetic hysteresis in the magnetic anisotropy, is of first order and is reversible with a hysteresis of ΔT about a mean transformation temperature T_0 . No change in saturation magnetization is observed through the transformation. The transformation is distinguished from relaxation phenomena in glasses⁵ by its discontinuous nature and by its unique kinetics which is described by an activation energy which decreases with increasing $|T - T_0|$ above or below

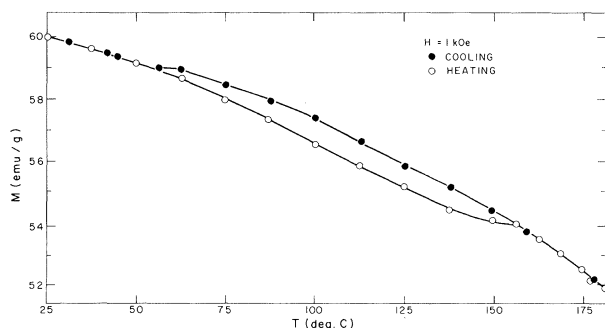


FIG. 1. Magnetization vs temperature for the glassy alloy $\text{Co}_{80}\text{Nb}_{14}\text{B}_6$ in an applied field of 1000 Oe.

T_0 . A model based upon changes in local cobalt-atom symmetry is proposed to explain the observations.

Figure 1 shows the magnetization as a function of temperature for $\text{Co}_{80}\text{Nb}_{14}\text{B}_6$ glass. The measurements were made in a vibrating-sample magnetometer with an applied field of 1000 Oe held parallel to the plane of the ribbon pieces. A scan rate of 0.5 deg/min was used. The loop can be retraced and the width ΔT of the hysteresis is proportional to the scan rate. The discrete difference in magnetization between the heating and cooling curves is caused by a difference in anisotropy⁶ between the high-temperature and low-temperature state of the glass. This is evident from Fig. 2 which shows two $M-H$ curves for the glassy CoNbB alloy taken at 75°C (cf. Fig. 1). The lower curve was obtained after heating from room temperature, while the upper curve was obtained after cooling from 200°C . Although both curves extrapolate to the same value of saturation magnetization, the greater magnetization (e.g., at 1000 Oe) of the cooling curve reflects

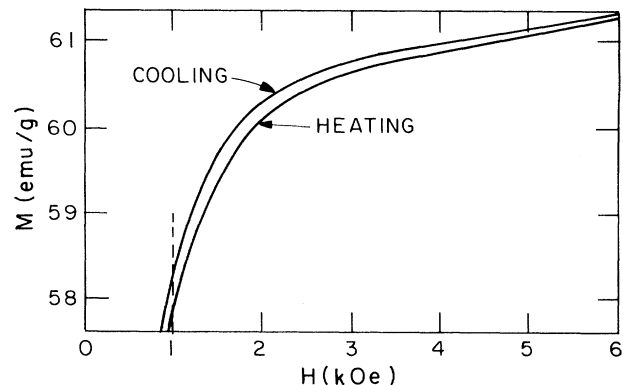


FIG. 2. Magnetization vs applied field at 75°C for the glassy CoNbB alloy of Fig. 1.

lower sample anisotropy energy.

The kinetics of transformation from one state to the other in Fig. 1 is shown in Fig. 3(a). The fractional change in magnetization varies as a function of time when the glassy alloy is held at a fixed temperature. Notice that the high-temperature state could not form until the temperature was greater than approximately $T_0 = 108^\circ\text{C}$. Similarly, the sample must be cooled below T_0 to nucleate the low-temperature state. Furthermore, the transformation rate in *either* direction is proportional to $|T - T_0|$. Empirically, it was found that the concentration of the parent phase c could be described by

$$d(\ln c)/dt = -A \exp(-Q/k_B T) \quad (1)$$

where it has been assumed that c is proportional to the fractional change in magnetization. The activation energies Q fitted to the data of Fig. 3(a) are shown in Fig. 3(b) as a function of $|T - T_0|$. Two additional Q 's are shown which were estimated from the time to transform at the extremities of the thermomagnetic hysteresis loop, hence their appreciable error bars. The observed activation energies Q are well described by

$$Q = Q_0 - Q_1 |T - T_0|, \quad (2)$$

where it was found that $Q_0 = 0.15 \pm 0.01$ eV and $Q_1 = (1.5 \pm 0.1) \times 10^{-3}$ eV/K.

First-order, displacive transformations in crystalline materials often show a temperature dependence of the effective activation energy that is similar to that described by Eq. (2) and is usually expressed as⁷

$$Q(T) = Q_0 + n^* \Delta g. \quad (3)$$

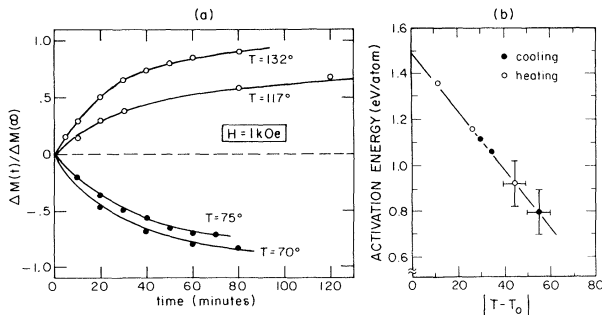


FIG. 3. (a) Isothermal transformation curves showing the fractional change in magnetization vs time for the glassy alloy of Fig. 1. (b) Dependence on $|T - T_0|$ of activation energies obtained from a fit to the data in (a) with Eq. (1).

Here n^* is the critical cluster size required to nucleate the transformation and Δg (< 0) is the free energy per atom driving the transformation. By substituting the thermodynamic relation $\Delta g = \Delta h - T\Delta s$ into Eq. (3) and using the entropy change for the hcp-fcc transformation in pure cobalt,⁸ $\Delta S = 0.15$ cal/mole K, we can estimate $n^* = 200$ atoms and $\Delta h = 60$ cal/mole K. This cluster is comparable in size to those for displacive transformations in crystalline transition metals and corresponds to a sphere of approximate diameter 17 Å. While the physical significance of this cluster size is not yet well understood, it need not be associated with the range of the local order. Rather it is more likely associated with the range over which a transformation at one site can couple coherently (by stress) to its neighbors. The heat of transformation observed by differential scattering calorimetry is only 9% of that estimated above from Eqs. (2) and (3). This suggests that not all of the glassy alloy is transforming. However, the volume fraction transforming is sufficiently large that if it were crystalline, it would be detectable by x-ray scattering. Our x-ray scattering experiments (sensitive to as little as 4% crystalline fraction) show no crystallinity. We conclude that the transformation is occurring in the glassy material itself if our estimated heat of transformation is correct to within a factor of 2.

Stronger evidence exists supporting the position that the transformation is occurring in the glassy material itself rather than only within microcrystallites which are known to be present in some as-prepared metallic glasses.⁹ Transmission electron microscopy (TEM) and scanning transmission electron microscopy (STEM) were performed on electropolished samples of our alloys. A typical dark-field TEM image of the $\text{Co}_{80}\text{Nb}_{14}\text{B}_6$ glassy alloy is shown in Fig. 4, left-hand side. The grainy "salt-and-pepper" pattern observed is characteristic of glassy materials and is almost identical to that seen in the readily-glass-forming PdSi alloys.¹⁰ For comparison, a dark-field TEM image of a $\text{Co}_{84}\text{Nb}_{10}\text{B}_6$ melt-spun alloy is shown in Fig. 4, right-hand side. Note the discrete 20 to 80 Å microcrystallites which fill approximately 10% by volume of the sample. STEM microdiffraction on these microcrystallites reveals discrete spots which can be indexed to reflections from various hcp and fcc planes (Fig. 4, patterns at lower right). In contrast only glassy halos (pattern at lower left) have been seen in microdiffraction from the $\text{Co}_{80}\text{Nb}_{14}\text{B}_6$ al-

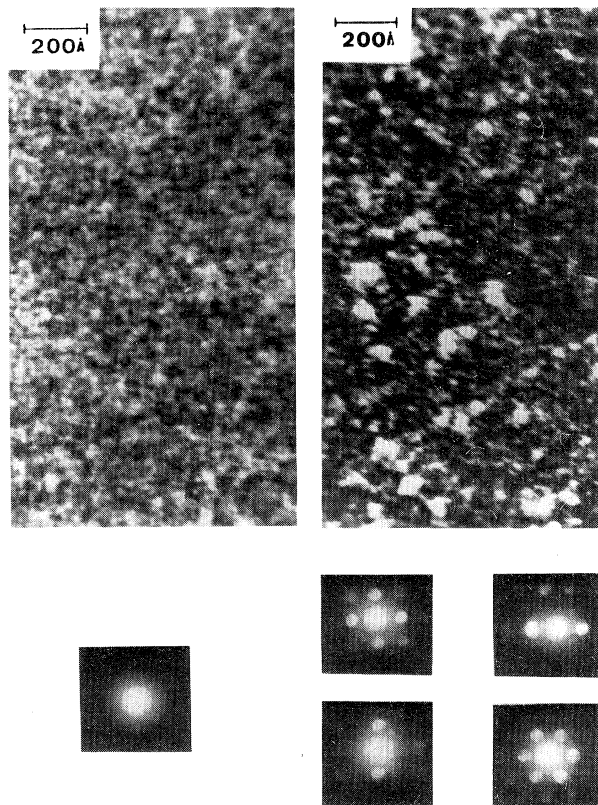


FIG. 4. TEM micrographs of $\text{Co}_{80}\text{Nb}_{14}\text{B}_6$ (left) and $\text{Co}_{84}\text{Nb}_{10}\text{B}_6$ (right) melt-spun alloys. Magnification is the same in both micrographs. A diffuse electron diffraction halo (left) is seen in STEM microdiffraction from the Co_{80} sample and from intercrystalline regions in the Co_{84} sample. Microdiffraction from the crystalline regions (Co_{84}) shows fcc and hcp diffraction patterns.

loys. Only the fully amorphous alloy shows a completely reversible transformation (Fig. 1). In the partially crystalline Co_{84} alloy the transformation observed from the low-temperature state to the high-temperature state (at approximately 180°C) was *not* able to be reversed upon returning to room temperature. Furthermore, when the glassy Co_{80} alloy was partially crystallized, the transformation was not observed at all. Thus, increasing the volume fraction of crystallinity in the alloy makes it increasingly difficult to transform the material.

Relaxation is a continuous transformation; the changes observed are between a continuum of states, depending on the temperature at which the sample is brought to equilibrium. Furthermore, the unique temperature at which $Q(T)$

peaks in relaxation is that of the glass transition T_g . The transformation described in this Letter is clearly between two discrete states; it is a first-order transformation showing a latent heat and a characteristic hysteresis. T_g was found to be greater than the crystallization temperature 470°C of our CoNbB glass,¹¹ and thus T_0 is well below T_g . These same arguments, plus the fact that the direction of the applied field was held constant during the thermal scans, rule out the possibility that the observed effects (Figs. 1 and 2) are due to an induced macroscopic anisotropy such as is the case in field annealing.

We therefore interpret the change in magnetic anisotropy in Fig. 1 as due to a discrete, first-order transformation between two different short-range orders in the glassy alloy. Because the saturation magnetization is insensitive to the transformation, the two states are probably characterized by the same overall coordination (chemical SRO) and differ mainly in their symmetry (topological SRO). The model which we propose to explain the observed effects assumes one local configuration, stable below T_0 , to be characterized by near-trigonal symmetry (stress-distorted building blocks of the hcp phase of crystalline cobalt-rich alloys) and another local configuration, stable above T_0 , to be characterized by near-octahedral symmetry (related to the fcc phase). These symmetries are readily obtained by small distortions of thirteen-atom clusters of icosahedral symmetry which, because of their local stability, are often used in modeling amorphous structures.^{12, 13}

It is suggested, then, that at room temperature a fraction of the glassy CoNbB alloy is comprised of randomly oriented clusters of near-trigonal symmetry (higher local magnetic anisotropy¹⁴ and lower magnetization at 1000 Oe). The remainder may be of icosahedral symmetry. At an elevated temperature, the higher-symmetry, near-octahedral clusters (lower local anisotropy and higher magnetization at 1000 Oe) become more stable. The presence of microcrystallites strains the structure to the extent that the transformation is inhibited.

We gratefully acknowledge helpful discussions with G. B. Olson. This work was supported by U. S. Army Research Office Grant No. DAAG-29-80-K-0088 and by the National Science Foundation under Grant No. DMR 81-19295 through MIT's Center for Materials Science and Engineering.

^(a)Present address: Institut für Physik der Universität Basel, Basel CH-4056, Switzerland.

¹P. H. Gaskell, *J. Phys. C* **12**, 4337 (1979); P. Panisod, D. Aliaga Guerra, A. Ammamou, J. Durand, W. L. Johnson, W. L. Carter, and S. J. Poon, *Phys. Rev. Lett.* **44**, 1465 (1980).

²C.-P. Chou and D. Turnbull, *J. Non-Cryst. Solids* **17**, 169 (1975); L. E. Tanner and R. Ray, *Scr. Metall.* **14**, 657 (1980); C. O. Kim and W. L. Johnson, *Phys. Rev.* **23**, 143 (1981); S. T. Hopkins and W. L. Johnson, *Solid State Commun.* **43**, 537 (1982).

³D. S. Lashmore, L. H. Bennett, H. E. Schone, P. Gustafson, and R. E. Watson, *Phys. Rev. Lett.* **48**, 1760 (1982).

⁴R. C. O'Handley and N. J. Grant, *Physica (Utrecht)* **119B**, 173 (1983); and T. Egami, *J. Magn. Magn. Mater.* **31-34**, 1571 (1983).

⁵H. S. Chen, in *Proceedings of the Fourth International Conference on Rapidly Quenched Metals*, edited by T. Masumoto and K. Suzuki (Japan Institute of Metals, Sendai, 1982), p. 495.

⁶Magnetic anisotropy is the energy required to orient the magnetization in a particular direction. Spin-orbit interaction and crystal-field symmetry determine the direction and strength of the local anisotropy, and in turn affect the macroscopic anisotropy. Consider, for example, the case of local uniaxial anisotropy $k_{10c} = k_1 \sin^2\theta + \dots$ randomly oriented throughout the sample. The macroscopic anisotropy $K = (4\pi)^{-1} \int k_{10c} d\Omega = (2/3)k_1 + \dots$ reflects the strength of the local aniso-

tropy.

⁷G. B. Olson and M. Cohen, *Metall. Trans.* **7A**, 1915 (1976), and in *Proceedings of the International Conference on Martensitic Transformations* (MIT, Cambridge, Mass., 1980), p. 310.

⁸L. Kaufman and H. Bernstein, *Computer Calculations of Phase Diagrams* (Academic, New York, 1970), p. 184. This calculated value for ΔS is close to that measured from stacking fault energies (G. B. Olson, private communication).

⁹Y. Ishida, H. Ichinose, H. Shimada, and H. Kojima, in *Proceedings of the Fourth International Conference on Rapidly Quenched Metals*, edited by T. Masumoto and K. Suzuki (Japan Institute of Metals, Sendai, 1982), p. 421.

¹⁰J. Megusar and N. J. Grant, *Mater. Sci. Eng.* **49**, 275 (1981).

¹¹R. C. O'Handley, B. W. Corb, Y. Hara, N. J. Grant, and W. A. Hines, *J. Appl. Phys.* **53**, 7753 (1982); R. C. O'Handley and N. J. Grant, in *Rapidly Solidified Amorphous and Crystalline Alloys*, edited by B. H. Kear, B. C. Giessen, and M. Cohen (Elsevier Sequoia, New York, 1982), p. 217.

¹²D. S. Boudreaux and H. J. Frost, *Phys. Rev. B* **23**, 1506 (1981).

¹³D. Mercier and J.-C. Levy, *Phys. Rev. B* **27**, 1292 (1983).

¹⁴M. Takahashi, S. Kadowaki, T. Wakiyama, T. Anayama, and M. Takahashi, *J. Phys. Soc. Jpn.* **44**, 825 (1978).

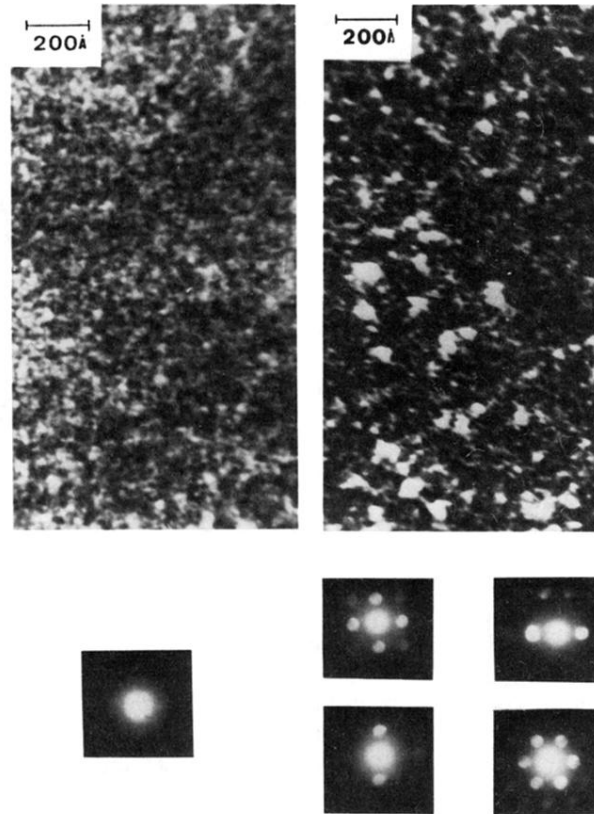


FIG. 4. TEM micrographs of $\text{Co}_{80}\text{Nb}_{14}\text{B}_6$ (left) and $\text{Co}_{84}\text{Nb}_{10}\text{B}_6$ (right) melt-spun alloys. Magnification is the same in both micrographs. A diffuse electron diffraction halo (left) is seen in STEM microdiffraction from the Co_{80} sample and from intercrystalline regions in the Co_{84} sample. Microdiffraction from the crystalline regions (Co_{84}) shows fcc and hcp diffraction patterns.